

Civil Engineering Journal

(E-ISSN: 2476-3055; ISSN: 2676-6957)

Vol. 11, No. 10, October, 2025



Performance Evaluation of Composite CNT/PE-Modified Asphalt Concrete at Binder, Mixture, and Pavement Levels

Amjad H. Albayati ¹ , Hasan Al-Mosawe ², Ahmed M. Maher ¹, Aliaa F. Al-Ani ¹, Mustafa M. Moudhafar ¹

¹ Department of Civil Engineering, University of Baghdad, Baghdad 10071, Iraq.

² Department of Civil Engineering, College of Engineering, Al-Nahrain University, Baghdad 10072, Iraq.

Received 19 May 2025; Revised 20 August 2025; Accepted 05 September 2025; Published 01 October 2025

Abstract

Advancing the multi-scale performance of asphalt pavements requires innovative binder modifications that address limitations in rutting resistance, fatigue resistance, and durability across the binder, mixture, and structural levels. This study evaluates the performance of asphalt cement, mixtures, and pavement systems modified with a combination of polyethylene (PE) and carbon nanotubes (CNTs). The binder was modified using 4% PE and varying CNT contents (0.5%, 1%, 1.5%, and 2% by weight of the modified binder). Binder performance was assessed through conventional and rheological tests, including penetration, softening point, viscosity, performance grade (PG) evaluation, and master curve analysis. Mixture-level performance was evaluated using Marshall properties, rutting, resilient modulus, and fatigue tests. Long-term pavement behavior was predicted using VESYS 5W software. The results showed that incorporating 1.0% CNT with 4.0% PE significantly improved binder rheology, increasing the true failure temperature by approximately 10% compared to the reference binder. Complex modulus and phase angle master curves also indicated notable improvements at low frequencies. Mixtures containing 2% CNT demonstrated approximately one-third of the permanent strain observed in the reference mix, while PCNT1.0% exhibited the best fatigue resistance. These findings highlight the significant role of combining plastomeric modifiers (PE) with nanoscale materials (CNTs) in enhancing the performance of asphalt binders and mixtures.

Keywords: Polyethylene; Carbon Nanotubes; Rutting; Fatigue; VESYS 5W.

1. Introduction

The continual demand for high-performance asphalt pavements, capable of withstanding increased traffic loads and severe environmental conditions, has spurred extensive research into advanced binder modification technologies. Traditional asphalt binders exhibit significant limitations such as thermal susceptibility, permanent deformation, and fatigue cracking, which compromise pavement durability and increase maintenance costs [1,2]. To mitigate these issues, the use of polymer-modified asphalts (PMAs) has gained widespread acceptance due to their ability to enhance both the rheological and mechanical behavior of asphalt binders [3, 4]. Among polymers, two principal classes are commonly utilized: elastomers and plastomers [5]. Elastomers are known for improving flexibility and fatigue resistance [6], while plastomers, particularly polyethylene PE, are effective in enhancing high-temperature performance by increasing the binder's softening point and stiffness, thereby reducing rutting potential [7]. PE-modified binders also offer advantages in terms of cost-effectiveness and ease of processing [8]. However, they often suffer from phase separation and reduced elasticity due to PE's limited compatibility with the asphalt matrix, leading to poor storage stability and compromised fatigue performance [9, 10].

^{*} Corresponding author: hasan.m.al-mosawe@nahrainuniv.edu.iq



doi http://dx.doi.org/10.28991/CEJ-2025-011-10-022

© 2025 by the authors. Licensee C.E.J, Tehran, Iran. This article is an open access article distributed under the terms and conditions of the Creative Commons Attribution (CC-BY) license (http://creativecommons.org/licenses/by/4.0/).

To overcome these limitations, nanomaterials have emerged as promising modifiers due to their high surface area, excellent mechanical strength, and thermal conductivity [11]. Nanomaterials can significantly improve the physical and chemical properties of asphalt binders by enhancing stiffness, elasticity, and resistance to oxidative aging [12]. Among these, carbon nanotubes (CNTs) have attracted considerable attention. With tensile strengths exceeding 100 GPa and remarkable thermal conductivity [13], CNTs offer a unique ability to reinforce the binder matrix at the molecular level, forming a rigid, interlocked network that resists deformation under mechanical stress [14].

Numerous studies have investigated the synergistic effect of combining nanomaterials with polymers, particularly in SBS-modified systems [15, 16]. The inclusion of nanoclay, nano-silica, and CNTs in SBS-PMAs has been shown to improve high- and low-temperature performance, enhance storage stability, and strengthen interfacial bonding between phases [17-19]. These improvements are attributed to the ability of nanoparticles to form bridging networks that restrict phase mobility and reinforce the binder structure [20]. However, comparatively fewer studies have focused on the use of nanomaterials with plastomer-based modifiers like PE. The non-polar, crystalline nature of PE presents dispersion challenges in the asphalt matrix; however, which nanomaterials can help overcome by improving compatibility and cohesion [21].

Recent investigations have demonstrated that combining CNTs with PE can produce binders with superior performance characteristics. For instance, Li and Tang [22] reported significant improvements in complex modulus and elastic recovery in CNT/PE-modified binders, attributing these effects to enhanced nano-scale dispersion and interfacial bonding. Similarly, Xin et al. [21] found that premixing CNTs with PE prior to blending with the binder improved rutting resistance, reduced phase angles, and enhanced aging resistance compared to systems where the modifiers were added separately. Furthermore, Liang et al. [23] showed that the combined use of the CNTs and PE leads to higher temperatures of softening point, lower penetration grade, and higher ductility of the asphalt binder. Also, improvement in moisture damage resistance was stated by the authors as compared to the neat asphalt binder. Table 1 summarizes selected previous studies compares them with the current study.

Table 1. Summary of previous studies

					В	Binder le	vel tes	t	M	lixture	level te	st
Ref.	Year	Binder type	Modifier content %	Main findings	Conventional tests	Storage stability	PG	Master curve	Marshall properties	Rutting	Resilient modulus	Fatigue test
[21]	2020	60-70 PEN	1% CNT, 4% PE	Found that premixing CNTs with PE prior to blending with the binder improved rutting resistance, reduced phase angles, and enhanced aging resistance compared to systems where the modifiers were added separately.	✓	✓	✓	✓	-	-	-	-
[23]	2020	50-70 PEN	0.5-1% CNT, 1-4% PE	Found that the combined use of the CNTs and PE leads to higher temperatures of softening point, lower penetration grade, and higher ductility of the asphalt binder.	✓	✓	✓	✓	✓	✓	✓	
[8]	2023	70-100 PEN	4% PE	PE-modified binders also offer advantages in terms of cost-effectiveness and ease of processing.	✓	-	-	-	✓	✓	✓	-
[13]	2022	60-70 PEN	0.1-1% CNT	Carbon nanotubes (CNTs) have attracted considerable attention. With tensile strengths exceeding 100 GPa and remarkable thermal conductivity.	✓	-	-	-	✓	✓	-	-
[22]	2023	-	1% CNT, 3-5% PE	Significant improvements in complex modulus and elastic recovery in CNT/PE-modified binders, attributing these effects to enhanced nano-scale dispersion and interfacial bonding.	✓	✓	✓	✓	✓	✓	-	-
[7]	2024	70-100 PEN	2-8% PE	Plastomers are effective in enhancing high-temperature performance by increasing the binder's softening point and stiffness, thereby reducing rutting potential.	✓	-	-	-	-	-	-	-
[14]	2024	40–50 PEN	0.5-1% CNT	CNTs offer a unique ability to reinforce the binder matrix at the molecular level, forming a rigid, interlocked network that resists deformation under mechanical stress.	✓	✓	✓	-	✓	✓	-	-
[4]	2024	70-100 PEN	4% PE	Ability to enhance both the rheological and mechanical behavior of asphalt binder.	✓	✓	-	-	✓	✓	✓	-
Current	2025	40-50 PEN	0.5-2% CNT, 4% PE	The addition of combined plastomers and nano size materials to improve asphalt binder and mixture performance.	✓	✓	✓	√	✓	✓	✓	✓

Despite these promising findings, comprehensive multi-scale studies evaluating the performance of CNT/PE-modified asphalt across the binder, mixture, and pavement levels remain limited. In particular, there is a lack of research on identifying the optimal CNT dosage in PE-modified binders to enhance pavement performance against

rutting and fatigue distresses. To address these gaps, the present study undertakes a systematic multi-scale evaluation of asphalt concrete modified with 4% polyethylene and varying carbon nanotube contents (0.5%, 1%, 1.5%, and 2% by weight of modified binder). This study included a series of laboratory tests, including penetration, softening point, viscosity, ductility, specific gravity, and storage stability, to evaluate the basic physical properties of the materials. Additional rheological tests, including a performance grade (PG) at high temperatures, frequency sweep, and a master curve over a wide temperature range, were conducted to study the viscoelastic behavior of the modified mixtures. In the next phase, performance tests were conducted on the asphalt mixtures, including resistance to permanent deformation, resilient modulus, and resistance to fatigue cracking, in addition to Marshall stability and flow tests. The results of these tests were combined to predict the long-term performance of pavements using VESYS 5W software. This integrated approach, illustrated in a diagram in Figure 1, aims to determine the optimal composition of asphalt mixtures that ensures maximum structural durability and long-term service efficiency and to contribute to the development of the next generation, high-performance asphalt pavement systems.

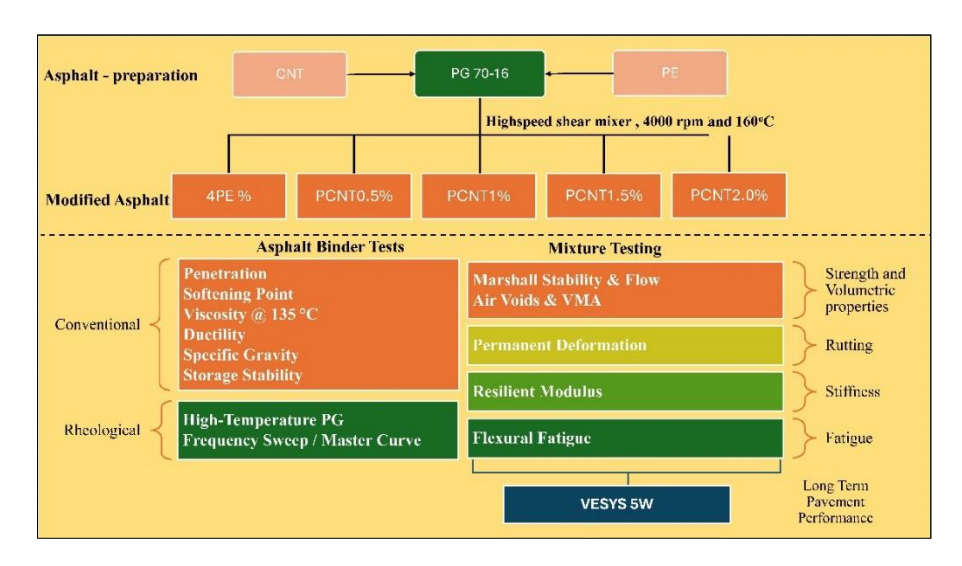


Figure 1. Experimental flowchart

2. Materials and Testing Program

2.1. Materials

2.1.1. Asphalt Binder

The implemented asphalt binder within the course of this work was obtained from the Doura Oil Refinery in Baghdad, Iraq. Table 2 summarizes its physical characteristics as determined by conventional penetration grading tests. Based on these results, the binder meets the specifications for AC 40–50 penetration grade in accordance with AASHTO M 20. Furthermore, its rheological behavior was investigated utilizing the Superpave Performance Grading (PG) system according to AASHTO M320. Table 3 shows the reference binder properties which confirm that the binder complies with the requirements for a PG 70-16 classification.

Property	Standard	Test result	Specification limit AASHTO M 20
Penetration at 25 $^{\circ}$ C,100 gm,5 sec. (0.1 mm)	AASHTO T 49	41	(40-50)
Ductility at 25 °C, 5 cm/min. (cm)	AASHTO T 51	110	>100
Flashpoint (Cleveland open cup), (°C)	AASHTO T 48	304	Min.232
Softening point, (°C)	AASHTO T 53	50.15	
Specific gravity at 25 °C	ASTM-D70	1.028	
The residue from rolling thin film oven test	AASHTO T 240		
Retained penetration,% of original	AASHTO T 49	58	≥55

Table 2. Reference asphalt binder properties

AASHTO T 51

70

>25

Ductility at 25 C, 5cm/min, (cm)

Table 3. PG Grading of reference asphalt binder

Asphalt cement	Properties	Temperature Measured °C	Measured Parameters	Specification Requirements, AASHTO M320-05	
	Flash Point (°C)	-	304	≥230 °C	
	Viscosity at 135 °C (Pa.s)	-	720	≤3000 m Pa.s	
0::1		58	7.553		
Original	PGP G/ 2 / 10 1/ (LP.)	64	3.917	- 1001B	
	DSR, G/sinδ at 10 rad/s (kPa)	70	1.768	≥1.00 kPa	
	-	76	0.855	_	
	Mass Loss (%)	-	0.262	≤1%	
Derec		64	6.334		
RTFO Aged	DSR, G/sinδ at 10 rad/s (kPa)	70	3.227	≥2.2 kPa	
	-	76		-	
	DGD G : 2 (10 1/ (1D))	28	3390	45000 1 P	
PAV	DSR, G.sinδ at 10 rad/s (kPa)	25	5142	≤5000 kPa	
Aged	BBR, Creep Stiffness (MPa)	-6	192	≤300 MPa	
	Slope m-value	-6	0.346	≥0.3	

2.1.2. PE and CNT

Ultra-high molecular weight polyethylene (UHMWPE) and multi-walled carbon nanotubes (MWCNTs) were employed as the primary modifiers in this study. UHMWPE, a subclass of polyethylene known for its exceptional tensile strength and thermal stability, was utilized in powder form to improve the stiffness and high-temperature performance of the asphalt binder. MWCNTs, characterized by their concentric cylindrical nanostructure, were selected for their superior mechanical properties, including high tensile strength and large specific surface area, which enable them to function as nanoscale reinforcement within the asphalt matrix. The key physical and chemical properties of both modifiers are summarized in Table 4. A photographic image of the materials, illustrating their morphology and physical appearance, is shown in Figure 2.

Table 4. Key features of PE and CNT

Material	Physical Form	Chemical Formula	Particle Size	Density (g/cm³)	Melting Point (°C)	Specific Surface Area (m²/g)	Purity (%)
PE	White Powder form	$(C_2H_4)_n$	120 μm	0.45	135	_	_
CNT	Black powder	C	20 nm diameter, 10 μm length	0.126	_	100–300	>95

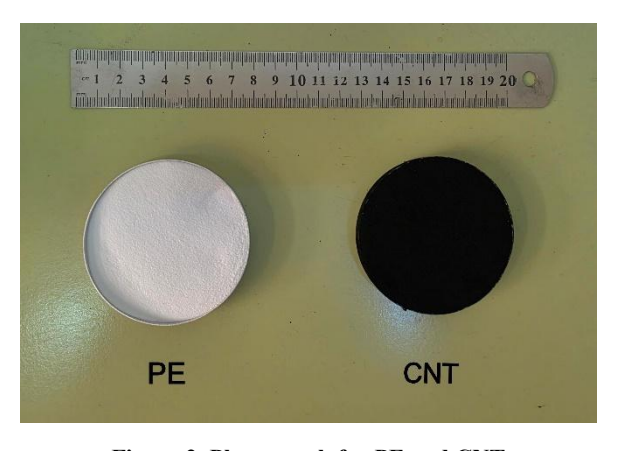


Figure 2. Photograph for PE and CNT

2.1.3. Aggregate and Mineral Filler

Crushed quartz aggregates were selected for this study, sourced from the Al-Nibaie quarry in the north of Baghdad. The aggregates were separated into coarse and fine fractions using a 4.75 mm (No. 4) sieve, then recombined to satisfy the aggregate gradation requirements for the D-5 mix type, as specified for wearing course applications in ASTM D3515, presented in Table 5 and shown graphically in Figure 3. The physical properties of the aggregates are summarized in Table 6, while the properties of the limestone filler used in the mixture are provided in Table 7.

Table 5. Aggregate gradation and specification limit

Sieve size (mm)	19	12.5	9.5	4.75	2.36	0.3	0.075
Gradation, %	100	95	83	59	37	13	7
ASTM D3515, D-5 limit, %	100	90-100	-	44-74	28 - 58	5 - 21	4 - 10

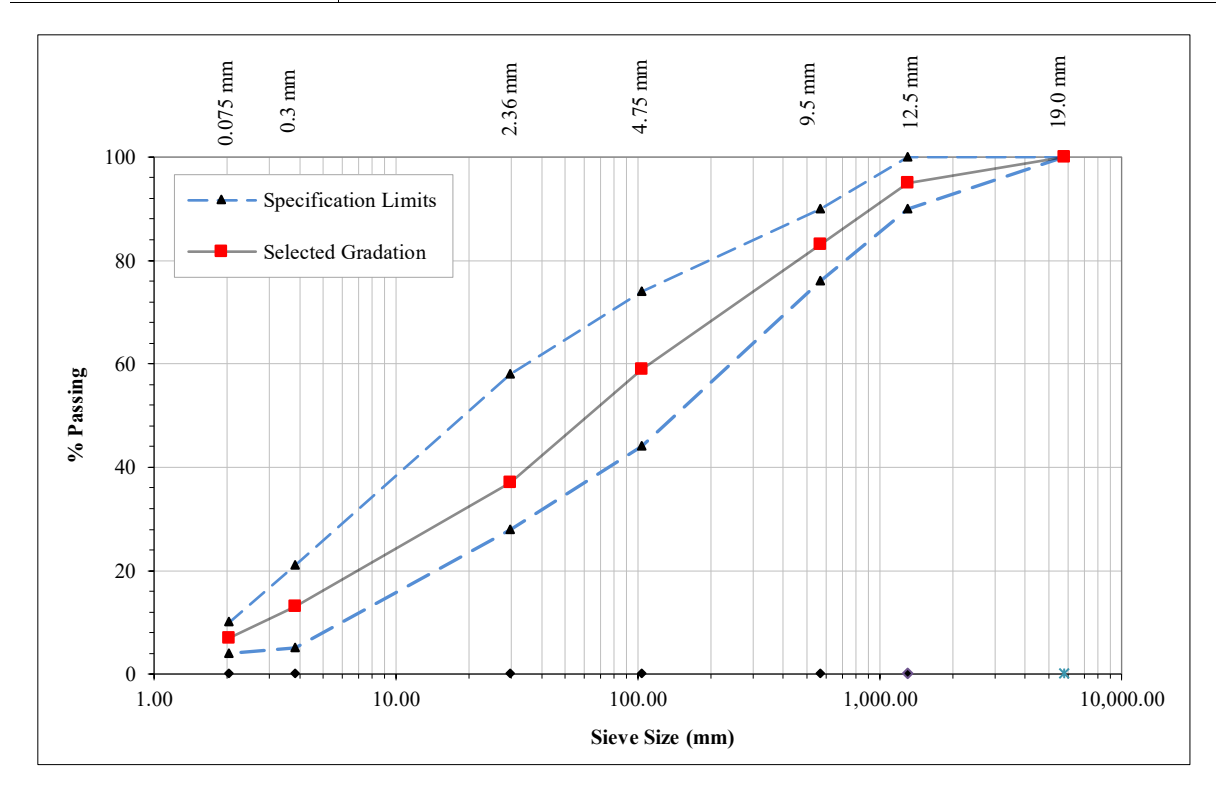


Figure 3. Aggregate gradation curve

Table 6. Physical properties of aggregate

Property	ASTM Designation	Test results	Specification requirement
	Coarse Aggregate		
Apparent Specific Gravity		2.709	-
Bulk Specific Gravity	C-127	2.628	-
Water Absorption, (%)		0.433	-
Soundness (Sodium Sulfate Solution Loss), (%)	C-88	4.8	12 max.
Percent Wear (Los Angeles abrasion), (%)	C-131	17	30 max.
Flat & Elongated (5:1), (%)	D4791	2	10 max.
Fractured Pieces, (%)	D5821	98	90 min.
	Fine Aggregate		
Apparent Specific Gravity		2.592	-
Bulk Specific Gravity	C-128	2.514	-
Water Absorption, (%)		0.988	-
Clay Lump and Friable Particles, (%)	C-142	1.26	3 max.
Sand Equivalent (%)	D2419	64	45 min.

Table 7. Physical properties of limestone filler

Specific Gravity	Surface Area (m²/kg)	Passing Sieve No. 200 (0.075), %
2.778	252	98

2.1.4. Modified Asphalt Binder Preparation Method

The modification process began by heating the base asphalt binder to $160\pm1\,^{\circ}\text{C}$ to reach the ideal mixing temperature. Once this temperature was stabilized, the binder was mixed for 20 minutes using a high-shear mixer to ensure uniform consistency. Polyethylene (PE) was then gradually incorporated into the binder at an elevated temperature of $160\pm1\,^{\circ}\text{C}$. The mixture was blended at a constant shear rate of 4000 rpm for 30 minutes using Jiffy head (shown in Figure 4) to promote proper dispersion and polymer interaction. Subsequently, carbon nanotubes (CNTs) were introduced at a controlled feed rate of 4 grams per minute. During CNT incorporation, mixing was maintained at 4000 rpm and $160\pm1\,^{\circ}\text{C}$ for an additional 30 minutes to ensure thorough and uniform distribution of the nanomaterial within the binder matrix. The selected mixing temperature and shear rate were adopted based on the methodology reported by Liang et al. [23], which demonstrated effective dispersion and stability of CNTs in polymer-modified asphalt systems.

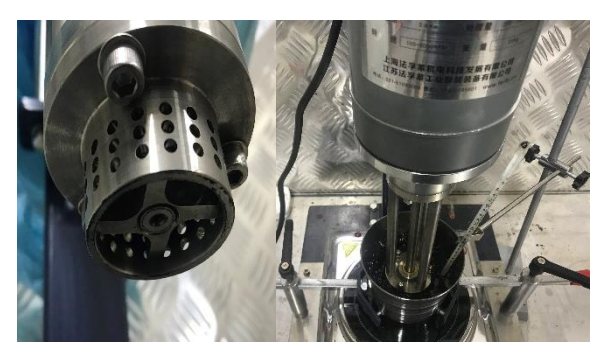


Figure 4. Blending of PE and CNTs with binder using high-shear mixer

To facilitate clarity throughout this study, a short legend system was used to identify each binder formulation: RB refers to the unmodified reference binder, PMB to the polymer-modified binder containing 4% PE, and PCNT0.5%, PCNT1%, PCNT1.5%, and PCNT2% denote the PE-modified binders with 0.5%, 1%, 1.5%, and 2% CNT additions, respectively.

2.2. Testing Program

2.2.1 Binder Tests

Binder performance was evaluated using both conventional and rheological tests to assess the effects of PE and CNT modifications. The conventional tests measured basic physical properties, while rheological evaluations were conducted to characterize viscoelastic behavior over a range of service temperatures. Number of samples for each test was three to ensure consistency and reliability of the results and the results were averaged and reported. A summary of the binder test methods is provided in Table 8.

Table 8. Binder tests description

			rable 8. Binder tests description	
Category	Test	Standard/ method	Test principle and conditions	Measurement / calculation
	Penetration	AASHTO T49	Assesses binder consistency using a needle under 100g load for 5s at 25°C.	Direct measurement (0.1 mm)
	Softening Point	AASHTO T53	Determines the softening temperature using the ring and ball method, heated at $\sim 5^{\circ}\text{C/min}$.	Direct measurement (°C)
Comment of the	Viscosity @ 135 °C	ASTM D4402	Evaluates mixing and compaction workability with Brookfield viscometer at 135°C.	Direct measurement (mPa·s)
Conventional	Ductility	AASHTO T51	Measures elongation before break at 25°C, pulled at 5 cm/min.	Direct measurement (cm)
	Specific Gravity	ASTM D70	Determines binder density using the pycnometer method at 25°C.	Direct measurement (g/cm³)
	Storage Stability	ASTM D7173	Evaluates phase separation after 48h storage at 163°C by comparing softening points.	Difference in softening point (°C)
	High-Temperature PG	AASHTO M320	Determines $G^*/\sin\delta$ for original binder using DSR from 58°C to 76°C at 10 rad/s.	G*/sinδ: ≥1.0 kPa (original)
Rheological	Frequency Sweep / Master Curve	AASHTO T315	DSR tests for RTFO aged samples at 30–70 °C with shift factors via WLF model (T_0 =50 °C); Master curve via CAM model.	$\begin{split} \log\alpha_t &= -[C_1(T-T_0)]/[C_2+(T-T_0)]\\ & G^* = \frac{G_g^*}{[1+(f_c/f_r)^k]^{(m/k)}}\\ \delta &= 90I - (90I-\delta_m) \bigg\{1+\bigg[\frac{\log(f_d/f_r)}{R_d}\bigg]^2\bigg\}^{-md/2} \end{split}$ where α_t is the shift factor, T: testing temperature, To is the reference temperature, and C_1, C_2 are fitting coefficients. G_g^* is the glass complex modulus, f_c is the crossover frequency, f_r is the reduced frequency, and m and k are the fitting parameters. δ_m is the phase angle at the inflection point f_d , with R_d and md as shape parameters, and $I=0$ if $I>f_d$ and $I=1$ if $I.$

2.2.2. Mixture Tests

Asphalt mixtures incorporating the modified binders were subjected to a comprehensive suite of mechanical tests to evaluate their structural performance. These tests included the determination of Marshall properties, assessment of permanent deformation resistance, measurement of resilient modulus, and evaluation of fatigue behavior. To enhance result reliability and account for experimental variability, all mixture tests were conducted in triplicate, with average values reported. Each test was selected to simulate specific loading and environmental conditions relevant to pavement performance. Table 9 presents a summary of the employed test methods, standards, and experimental conditions used in the evaluation.

Table 9. Asphalt Mixture Testing Protocol

Category	Test	Standard /Method	Test Principle and Conditions	Measurement / Calculation		
	Marshall Stability & Flow	ASTM D6927-15	Evaluates plastic flow resistance and deformation using Marshall apparatus. Specimens compacted (75 blows/side), immersed in water for 45 min before testing.	Stability = peak load (kN), Flow = deformation at max load (mm)		
Strength and Volumetric properties	Air Voids & VMA	ASTM D2726-04, D2041-11	Determines air voids and voids in mineral aggregate using bulk and theoretical specific gravity values.	230		
Rutting	Permanent Deformation	AASHTO T 378	Cylindrical specimens (100 mm dia. \times 200 mm height) loaded uniaxially at 40 °C under 0.137 MPa stress, 1 Hz rectangular waveform (0.1s load, 0.9s rest). The specimen air voids content 7 \pm 1%.	$p_d \times 10^6$		
Stiffness	Paciliant AASUTO Same cetup at 20°C Paciliant deflection		Same setup at 20 °C. Resilient deflection measured at 50–100 cycles.	$\begin{split} \varepsilon_r &= \frac{r_d \times 10^6}{h} \\ M_r &= \frac{\sigma}{\varepsilon_r} \\ where: rd is the axial resilient deflection; h is the height of the specimens (mm); and \sigma is axial stress$		
Fatigue	Flexural Fatigue	Third-Point Bending Test	Beam specimens ($76\times76\times381$ mm) tested at 20 °C under 20 Hz loading (0.1s load, 0.4s rest). The specimen air voids content $7\pm1\%$.	$\epsilon_t = \frac{12h\Delta}{3L^2 - 4a^2}$ where: ϵt is the initial tensile strain, h is the height of the specimens (mm), Δ is recorded flexural deformation at the center of the specimen, L is the span between the two supports of the beam, a is the distance from the load to the support (beam length over three)		

2.2.3. Mixture Design

The Marshall mix design methodology was utilized to ascertain the optimum asphalt content (OAC) for the reference mix incorporating RB. A total of five asphalt contents; 4.0%, 4.5%, 5.0%, 5.5%, and 6.0% by weight of the total mix were evaluated. For each binder content, specimens were prepared and tested in accordance with ASTM D6927 to determine Marshall stability, flow, bulk specific gravity, air voids (VTM), and voids in mineral aggregate (VMA). The maximum theoretical specific gravity (Gmm) was measured following ASTM D2041, and bulk specific gravity (Gmb) according to ASTM D2726. The optimum binder content was identified as the average asphalt content corresponding to: (1) the maximum stability, (2) the maximum density, and (3) an air void level closest to 4%. Based on the results summarized in Table 10, the OAC was determined to be 5.0%, which achieved peak stability (10.56 kN), acceptable flow (3.48 mm), and an air void content of 4.02%, all of which meet the specified criteria. The VMA at this binder content was also within specification (>14%), indicating a well-balanced mix design. To ensure consistency across all modified mixtures incorporating PE and CNTs, this optimum binder content of 5.0% was maintained throughout the study, rather than recalculating the OAC for each individual modification.

Table 10. Marshall mix design results

Asphalt Content (%)	Stability (kN)	Flow (mm)	Unit Weight (g/cm³)	Gmm	VTM (%)	VMA (%)
4.0	5.99	2.02	2.2525	2.4398	7.67	16.54
4.5	7.94	2.65	2.3097	2.4398	5.33	15.15
5.0	10.56	3.48	2.3418	2.4398	4.02	14.59
5.5	9.41	3.89	2.3367	2.4297	3.83	14.69
6.0	8.27	4.26	2.3277	2.4146	3.60	14.96

3. Results and Discussion

3.1. Binder Results

3.1.1. Conventional Test Results

Figure 5 illustrates the influence of PE and CNT modifications on the conventional properties of asphalt binders, including penetration, softening point, viscosity, ductility, specific gravity, and storage stability. The incorporation of 4% PE into the RB substantially reduced the penetration value by 31.7%, indicating an increase in stiffness, while simultaneously elevating the softening point by 11.9%, which reflects enhanced thermal resistance. This aligns with previous findings stated by Yang et al. [4], who described PE modification as a physical interaction where PE absorbs lighter maltene fractions from the binder, resulting in a phase-separated structure that improves high-temperature performance.

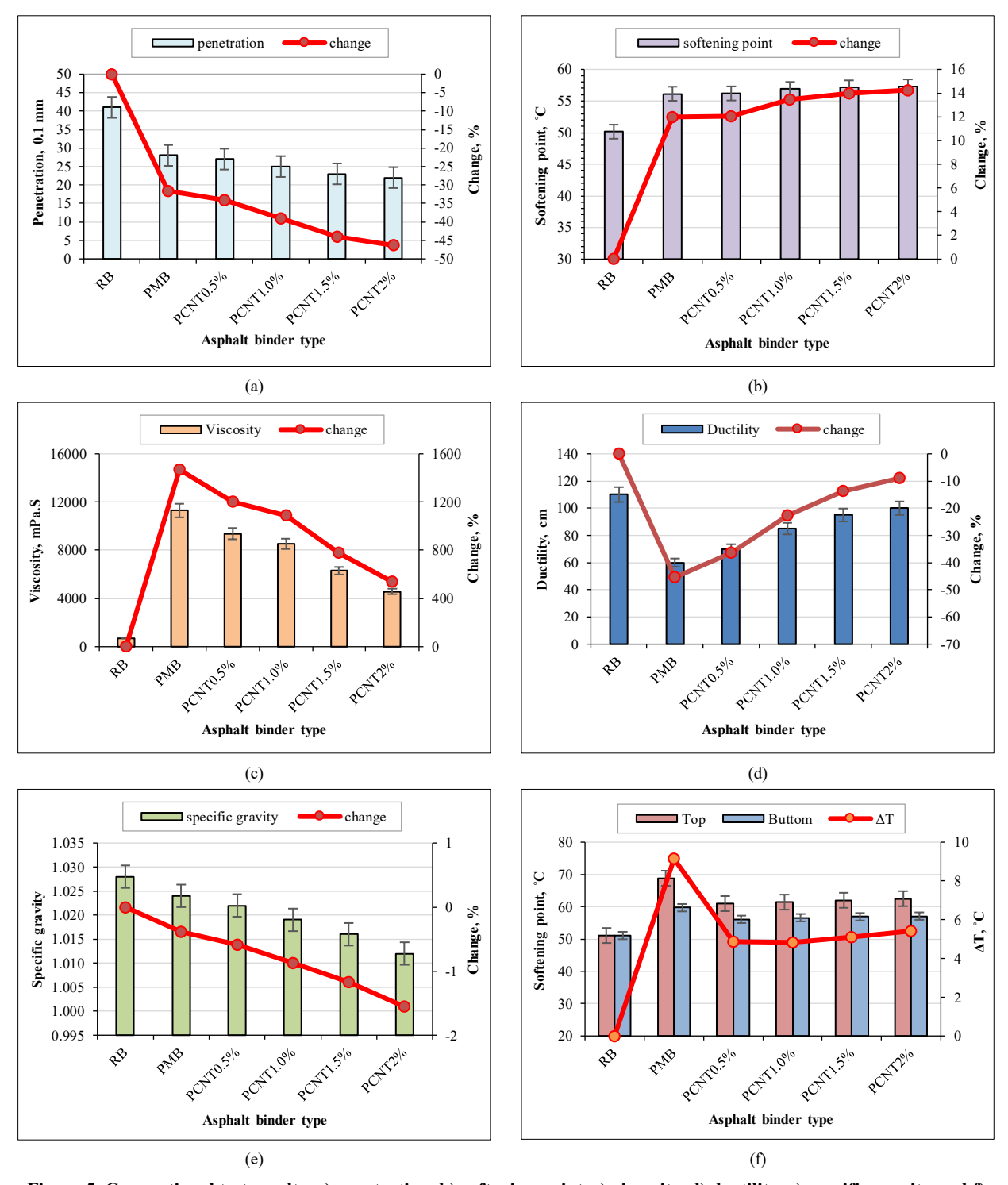


Figure 5. Conventional test results, a) penetration, b) softening point, c) viscosity, d) ductility, e) specific gravity and f) storage stability

However, as CNTs were incrementally introduced (from 0.5% to 2%), the penetration continued to decline, showing a cumulative stiffening effect, whereas the softening point increased only marginally, suggesting diminishing returns in thermal enhancement. Interestingly, viscosity at $135\,^{\circ}$ C displayed a non-monotonic trend. While the PMB exhibited a sharp increase in viscosity (~1468%), the addition of CNTs led to a progressive decrease. This behavior can be attributed to the nanoscale dimensions of CNTs, which, at elevated temperatures, disrupt the PE's capacity to absorb light fractions by interfering with the physical entrapment mechanism, thus reducing the viscosity despite increased solid content. Ductility results revealed a substantial initial drop with PE (~45.5%), indicating reduced elasticity, but partial recovery was observed with CNT incorporation. This improvement is attributed to enhanced dispersion and the formation of a nano-network that facilitates limited flexibility within the binder matrix. Specific gravity showed a slight decreasing trend with increasing CNT content, likely reflecting the lower bulk density of CNTs. The most notable improvement was observed in storage stability. In PMB, phase separation was evident with a top-bottom softening point difference (Δ T) of 9.13 °C. Upon CNT addition, Δ T was significantly reduced and stabilized around 5 °C, indicating a more homogeneous and thermally stable system. This stabilization is likely due to the interaction of CNTs at the PE–asphalt interface, which enhances interfacial adhesion and limits polymer agglomeration, thereby mitigating phase separation during storage.

3.1.2. High Temperature PG Results

The high performance grade outcomes, derived from the rutting parameter (G*/sin δ) measurements, are illustrated in Figure 6, while the corresponding true failure temperatures for each binder are summarized in Table 10. The reference binder (RB) recorded the lowest pass/fail temperature of 74.2 °C, indicating its limited resistance to permanent deformation under elevated temperatures. Upon incorporating 4% polyethylene, the PMB formulation improved substantially, achieving a true fail temperature of 79.2 °C. This enhancement reflects the contribution of PE in forming a rigid polymer network that improves high-temperature stiffness and delays rutting onset. Further modification with carbon nanotubes (CNTs) led to an incremental rise in performance. As shown in Table 11, PCNT0.5%, PCNT1.0%, PCNT1.5%, and PCNT2.0% exhibited pass/fail temperatures of 80.3 °C, 81.5 °C, 81.2 °C, and 80.9 °C, respectively. Notably, the addition of 1.0% CNT led to an increase of approximately 10% in the fail temperature compared to the reference binder, indicating a pronounced improvement in high-temperature rheological properties. This enhancement can be attributed to the optimal dispersion and reinforcing action of CNTs within the PE matrix. However, a marginal decrease at higher CNT contents (1.5% and 2%) suggests that excessive CNTs may induce particle agglomeration or matrix stiffening beyond the effective threshold, limiting additional rheological benefits. Overall, these findings confirm that CNTs enhance the high-temperature performance of PE-modified asphalt binders, with 1.0% CNT offering the most favorable outcome.

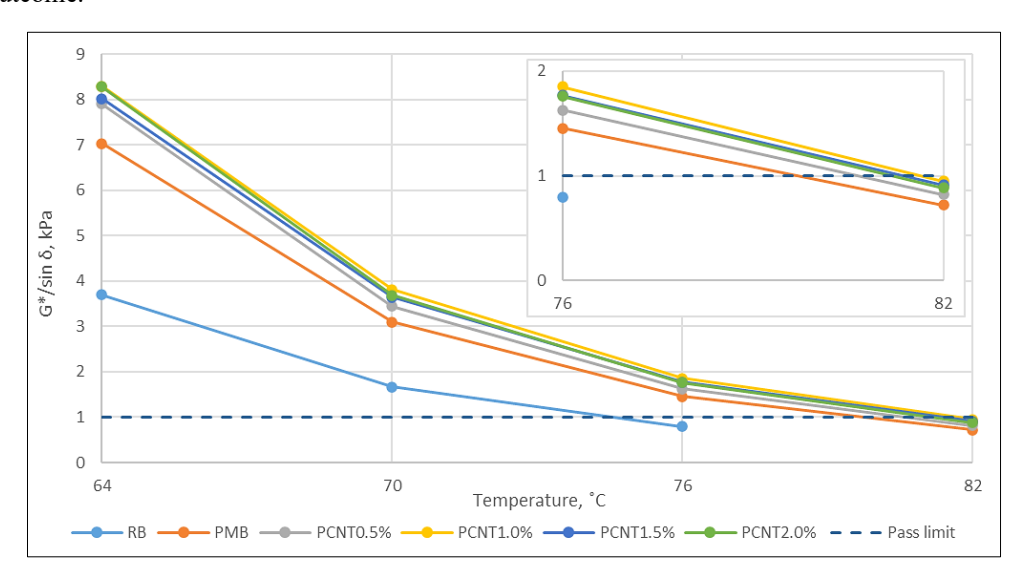


Figure 6. $G^*/\sin\delta$ for different binder types

Table 11. Binders pass/fail temperature

Binder	True fail temperature (°C)
RB	74.2
PMB	79.2
PCNT0.5%	80.3
PCNT1.0%	81.5
PCNT1.5%	81.2
PCNT2.0%	80.9

3.1.3. Master Curve Diagrams

Figures 7 and 8 present the master curves derived from frequency sweep test of complex shear modulus ($|G^*|$) and phase angle (δ), respectively, for the unmodified and modified asphalt binders, constructed at a reference temperature of 50 °C using the time–temperature superposition principle. These curves provide a comprehensive assessment of the binders' viscoelastic behavior over a wide range of reduced frequencies. As shown in Figure 7, the incorporation of 4% PE (PMB) significantly shifted the $|G^*|$ curve upward relative to the reference binder (RB), indicating a notable enhancement in stiffness across all frequency ranges. Further increases were observed with the addition of CNTs up to 1.0%, with PCNT1.0% exhibiting the highest modulus at low frequencies, indicative of superior rutting resistance under prolonged loading or high-temperature conditions. However, beyond 1.0% CNT, the increase in stiffness plateaued, suggesting a saturation effect where additional CNTs contributed marginally to the stiffness improvement, possibly due to particle agglomeration that limits their reinforcing efficiency.

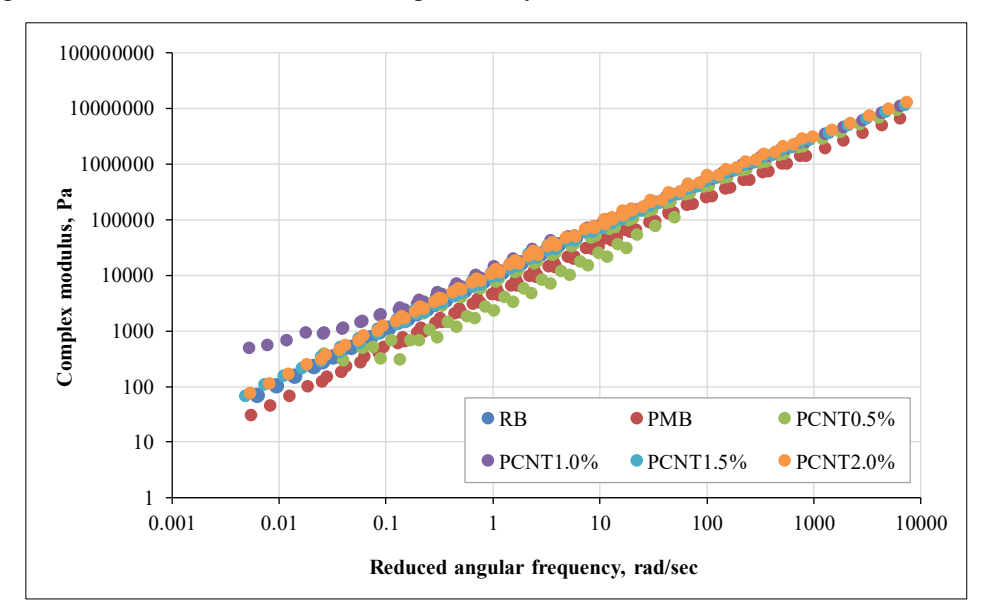


Figure 7. Master curve of G* for different binder types

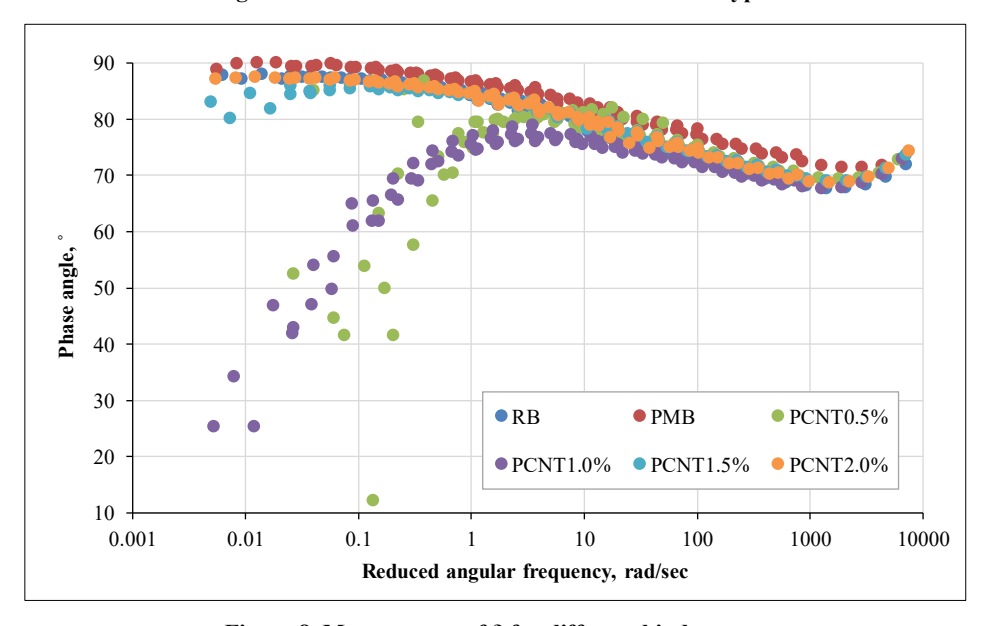


Figure 8. Master curve of $\boldsymbol{\delta}$ for different binder types

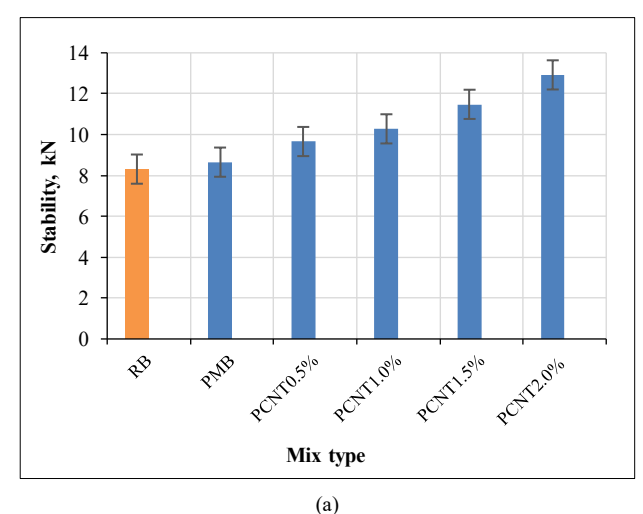
The phase angle master curves in Figure 8 reveal complementary trends. The RB exhibited the highest δ values across most frequencies, denoting a predominantly viscous behavior. The addition of PE decreased the phase angle, reflecting a shift toward more elastic performance. With CNT inclusion, particularly at 1.0% and higher, δ values further declined, particularly in the intermediate and low-frequency regions. This indicates an enhanced elastic response and reduced energy dissipation, which are beneficial for resisting permanent deformation. Interestingly, the curve for PCNT1.0% displayed the most pronounced reduction in phase angle, suggesting optimal network formation and stress transfer capability within the modified binder. These trends are consistent with the improved high-temperature performance observed in the PG grading (Table 11), affirming the synergistic effect of CNTs and PE in enhancing both stiffness and elasticity.

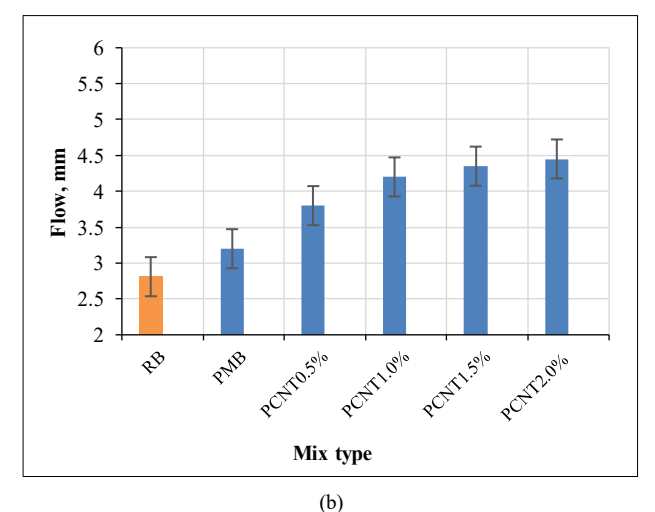
3.2. Mixture Test Results

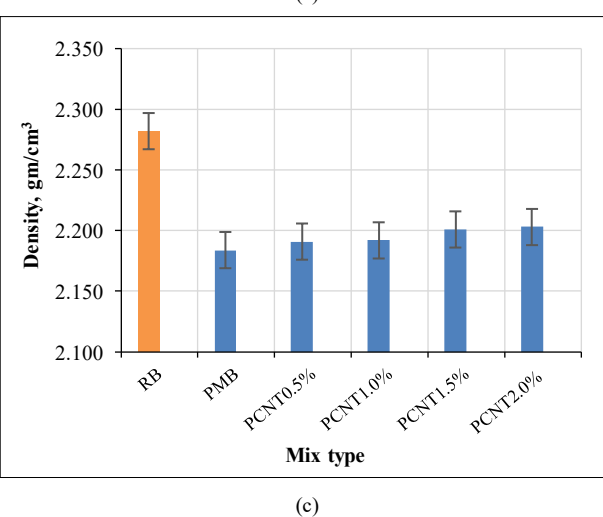
3.2.1. Marshall Properties

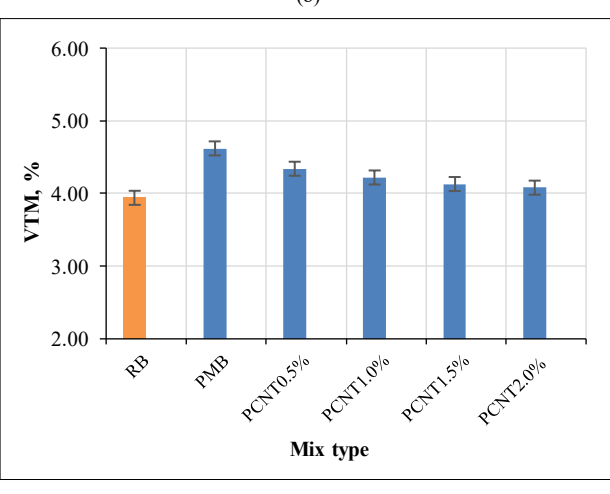
The effects of different binders on the Marshall properties of asphalt mixtures, including stability, flow, bulk density, air voids (VTM), and voids in mineral aggregate (VMA), are presented in Figure 9. The incorporation of PE and CNTs led to a consistent improvement in Marshall stability. While the RB exhibited a stability of 8.31 kN, this value increased to 8.65 kN with the polymer-modified binder (PMB) and peaked at 12.92 kN with the addition of 2.0% CNTs. This improvement highlights the synergistic effect of PE and CNTs in enhancing internal cohesion and load-bearing capacity. The increased rigidity and interlocking within the mastic matrix likely contribute to the enhanced resistance to plastic deformation. Marshall flow values also increased with CNT content, rising from 2.81 mm (RB) to 4.45 mm (PCNT2.0%). This behavior suggests that although the mixtures became stiffer, they retained sufficient flexibility to distribute stress without premature cracking. In terms of density, mixes with RB showed the highest value (2.282 g/cm³), while modified mixtures exhibited slightly lower but progressively increasing densities with CNT addition—reflecting the densifying effect of CNTs due to improved packing and matrix uniformity.

The VTM rose from 3.94% (RB) to 4.62% in PMB, primarily due to the higher stiffness of the PE-modified binder, which reduced compaction efficiency. However, with the incremental addition of CNTs, VTM values declined, indicating enhanced workability and better aggregate interlock, leading to a more tightly packed structure. VMA exhibited a distinct trend. It increased notably from 14.78% in RB to 17.8% in PMB, a result of the elevated stiffness and viscosity introduced by PE, which hindered aggregate compaction and promoted intergranular voids. However, as CNT content increased from 0.5% to 2.0%, VMA gradually declined. This inverse relationship between VMA and CNT dosage, coupled with the reduction in VTM, suggests that CNTs improved binder mobility and void filling capability. These findings are consistent with the binder-level viscosity trends, where the sharp viscosity increase caused by PE was partially mitigated by CNTs. At the mixing temperature (135 °C), the nanoscale structure of CNTs likely disrupted the physical entrapment mechanism of PE, lowering viscosity and enhancing binder flow. This improved workability allowed better coating of aggregates, reduced entrapped air, and facilitated denser packing. Consequently, the synergistic interaction between PE and CNTs not only strengthens the mix mechanically but also enhances its compactability and internal cohesion.









(d)

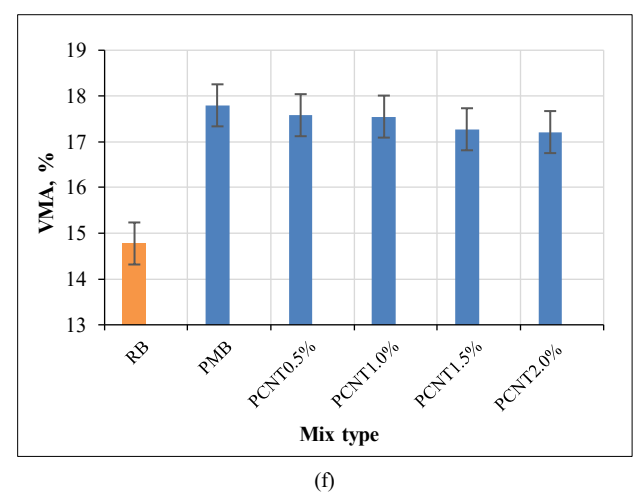


Figure 9. Effect of binder types on Marshall properties results, a) stability, b) flow, c) density, d) VTM and e) VMA

3.2.2. Permanent Deformation

The accumulation of permanent strain under repeated loading is often modeled using a power-law relationship as expressed in Equation 1.

$$\mathcal{E}_{\mathbf{p}} = aN^b \tag{1}$$

where ϵp is the accumulated permanent strain, N is the number of load cycles, and a and b are material constants. As shown in Figure 10, this relation produced a linear trend on the logarithmic scale, allowing the interpretation of a (intercept) as the initial strain at N = 1 and b (slope) as the rate of strain accumulation. Lower values of both parameters indicate enhanced rutting resistance.

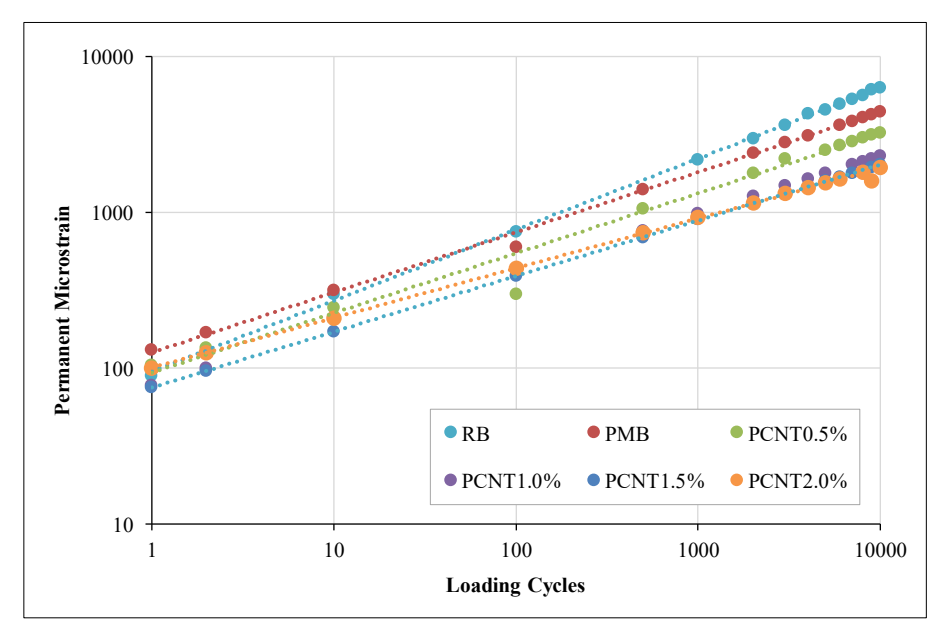


Figure 10. Accumulated permanent strain vs. loading cycles

According to the results summarized in Table 12, the mix with RB showed the highest permanent strain after 10,000 cycles (6296 μ_{ϵ}), consistent with its lowest stiffness and resistance to plastic flow. The addition of PE (PMB) significantly reduced the accumulated strain to 4435 μ_{ϵ} and decreased the strain rate parameter b from 0.4612 (RB) to 0.3824, demonstrating the beneficial effect of polyethylene in improving high-temperature performance. Further enhancements were observed with CNT incorporation. The mix with 2% CNTs (PCNT2.0%) achieved the lowest strain (1948 μ_{ϵ}), approximately one-third of the strain observed in the RB, while also demonstrating the flattest accumulation slope (b=0.3224), highlighting the superior rutting resistance achieved through CNT reinforcement. This improvement is attributed to the nano structural interlocking of CNTs within the mastic matrix, which restricts binder mobility and enhances the load distribution across the aggregate skeleton. Additionally, the progressive decline in both (a) and (b) with increasing CNT content confirms the efficiency of PE/CNT synergy in mitigating permanent deformation. While

PCNT2.0% exhibited a slight increase in initial strain value (a=100) compared to PCNT1.5% (a=75), its improved resistance to long-term strain accumulation underscores its effectiveness at higher stress durations. Overall, the combined use of PE and CNTs delivers a significant enhancement in rutting resistance, positioning these binders as promising alternatives for high-performance asphalt pavements exposed to heavy traffic loads and elevated temperatures.

A b -14	Permanent deformation parameters						
Asphalt mix	I	S	(ϵ_p) at N = 10,000, microstrain				
RB	90	0.4612	6296				
PMB	131	0.3824	4435				
PCNT0.5%	104	0.3742	3265				
PCNT1.0%	78	0.3677	2306				
PCNT1.5%	75	0.3582	2032				
PCNT2.0%	100	0.3224	1948				

Table 12. Permanent deformation parameters

3.2.3. Resilient Modulus

The resilient modulus (Mr) results depicted in Figure 11 illustrate how binder modifications influence the elastic recovery characteristics of asphalt mixtures under repeated loading at $20\,^{\circ}$ C. Across all modified mixtures, Mr values exceeded that of the reference binder (RB), which recorded the lowest stiffness (\$\approx 2650 MPa)\$. This highlights the limited ability of the unmodified binder to resist repeated traffic-induced stresses. Incorporation of polyethylene (PMB) resulted in a notable increase in modulus (\$\approx 3000 MPa)\$, attributed to the enhanced rigidity and matrix reinforcement provided by the plastomer. When CNTs were further introduced into the PE-modified system, a dose-dependent trend emerged. Mr values increased progressively up to 1.0% CNTs (peaking at \$\approx 3340 MPa)\$, beyond which a slight decline was observed for higher dosages (PCNT1.5% and PCNT2.0%).

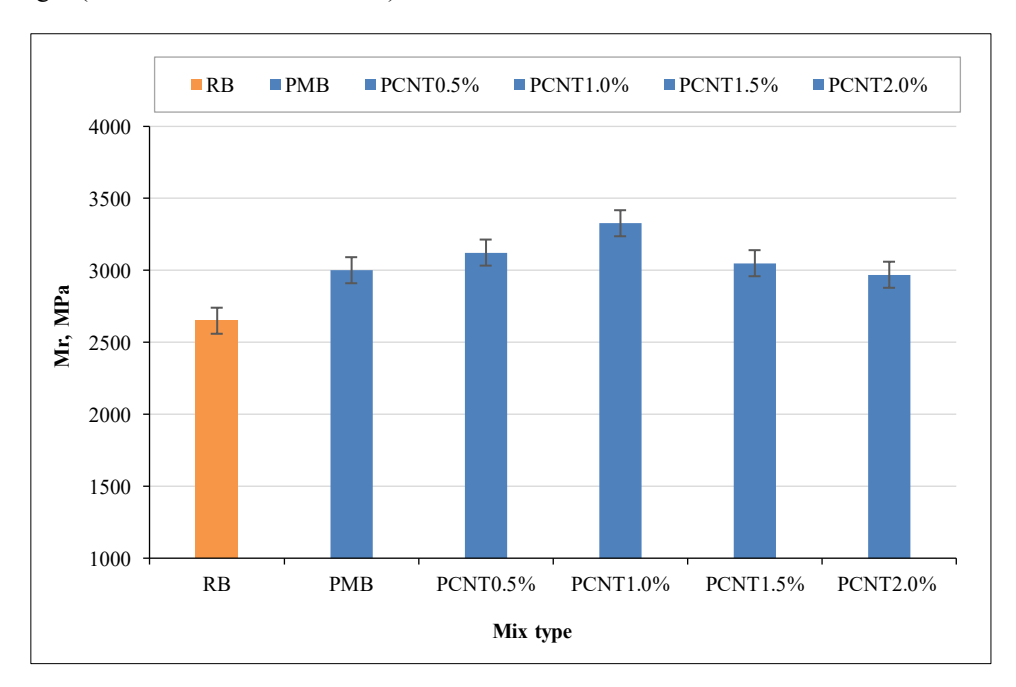


Figure 11. Mr results for mixtures with different binder types

This non-linear response suggests that moderate CNT content contributes effectively to reinforcing the mastic phase by improving stiffness and elastic recovery, likely through enhanced load transfer mechanisms and internal friction. However, higher CNT dosages may introduce dispersion challenges or localized agglomeration, disrupting the uniform binder-filler interaction and leading to diminished mechanical coherence. Importantly, these results do not merely reflect changes in stiffness but also imply structural integrity at the microscale. The optimized mix (PCNT1.0%) demonstrates the highest resilient modulus, indicating enhanced stiffness and elasticity under repeated loading. This suggests an effective balance between structural reinforcement from CNTs and the ability to maintain load recovery performance without inducing excessive brittleness or compromising mixture integrity.

3.2.4. Flexural Fatigue

The flexural fatigue behavior of asphalt mixtures was evaluated using a repeated loading bending beam configuration based on the classical fatigue model:

$$N_{f\vec{\epsilon}} = k_1(\varepsilon_t)^{-k2} \tag{2}$$

where N_f is number of load cycles to failure, ε_t is initial tensile strain (microstrain), K_1 is fatigue coefficient, representing the estimated fatigue life at unit strain, K_2 is fatigue exponent (inverse slope), indicating the sensitivity of fatigue life to strain level.

This model establishes a log-log linear relationship between initial tensile strain and fatigue life, as illustrated in Figure 12. A higher k1 implies better resistance to fatigue damage, while a lower k_2 suggests that fatigue life is less sensitive to variations in tensile strain, both of which are desirable traits for durable pavements. As shown in Table 13, the reference binder (RB) mixture exhibited the highest fatigue coefficient (k1=6.842E-07) but the lowest slope value (k_2 =2.284), indicating relatively better performance at very low strain levels but poor durability under moderate to high strains. The PMB mixture showed a slightly reduced k_1 , but a moderately improved k_2 =2.796, reflecting enhanced performance under increased loading cycles

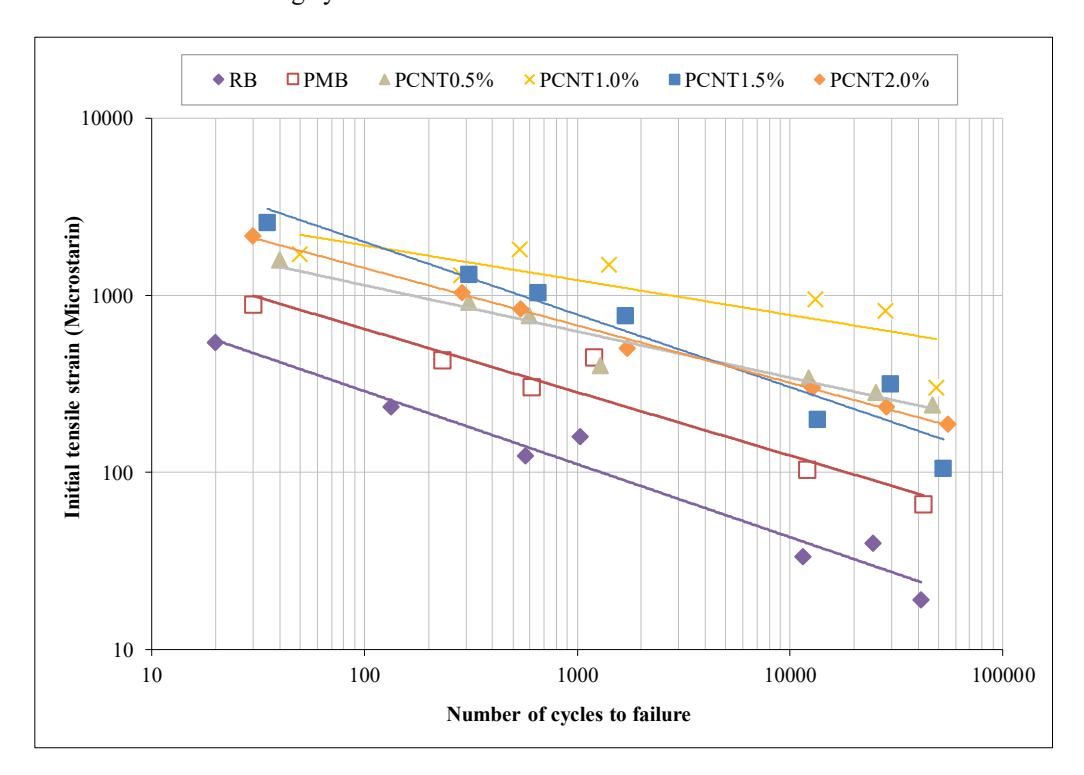


Figure 12. Fatigue performance for mixtures with different binder types

Table 13. Fatigue test results

Mix Type	RB	PMB	PCNT0.5%	PCNT1.0%	PCNT1.5%	PCNT2.0%
k_1	6.842E-07	9.024E-08	1.157E-09	1.144E-11	1.685E-07	1.812E-07
k_2	2.284	2.796	3.760	4.988	3.213	3.083

Notably, the PE/CNT-modified mixtures displayed significant variation in fatigue response. PCNT1.0% achieved the most balanced fatigue resistance with a steep slope k_2 =4.988, indicating strong endurance under fluctuating strains, although its k_1 value was lower (1.144E-11), potentially due to stiffening at low strain levels. Other mixes, such as PCNT1.5% and PCNT2.0%, also demonstrated improved k_2 values (3.213 and 3.083 respectively), showing greater fatigue tolerance relative to RB and PMB. Figure 13 offers a visual overview of the fatigue test setup and failure mechanisms, as seen in Figure 13-c, fatigue failure typically initiated with a narrow surface-level crack, which then propagated rapidly under repeated loading. The PCNT1.0% mixture exhibited delayed macrocrack formation, consistent with its lower fatigue slope, supporting the hypothesis that CNTs enhance the internal cohesion of the binder matrix.

This crack-bridging effect likely retards both crack initiation and propagation by distributing strain more effectively. Overall, the synergistic inclusion of PE and CNTs positively influenced fatigue behavior, particularly at an optimal CNT dosage of 1.0%. However, higher dosages (e.g., PCNT2.0%) may lead to over-stiffening, reducing flexibility and ultimately diminishing fatigue life under cyclic loading.



Figure 13. Fatigue test, a) specimen while testing, b) support positioning, c) failure commencement

Overall, the synergistic inclusion of PE and CNTs appears to positively influence fatigue behavior up to an optimal dosage. CNTs may improve stress distribution and microcrack resistance through network reinforcement, especially at intermediate concentrations. However, at high dosages (e.g., PCNT2.0%), over-stiffening effects may limit flexibility, reducing fatigue life under repeated loading.

3.3. Performance Prediction using VESYS 5W

To evaluate the long-term performance of asphalt pavements incorporating PE and CNT-modified binders, VESYS 5W software was employed. The pavement structure used in the simulation is illustrated in Figure 14, comprising a 100 mm thick asphalt concrete wearing course placed over a 350 mm granular subbase, underlain by a compacted subgrade. The Poisson's ratio was assumed to be 0.35 for the asphalt layer, 0.45 for the subbase, and 0.50 for the subgrade. The resilient modulus (Mr) values for subbase and subgrade were set at 206.9 MPa and 34.4 MPa, respectively, while the Mr for the asphalt layer was varied according to the mix type, reflecting binder-specific stiffness behavior.

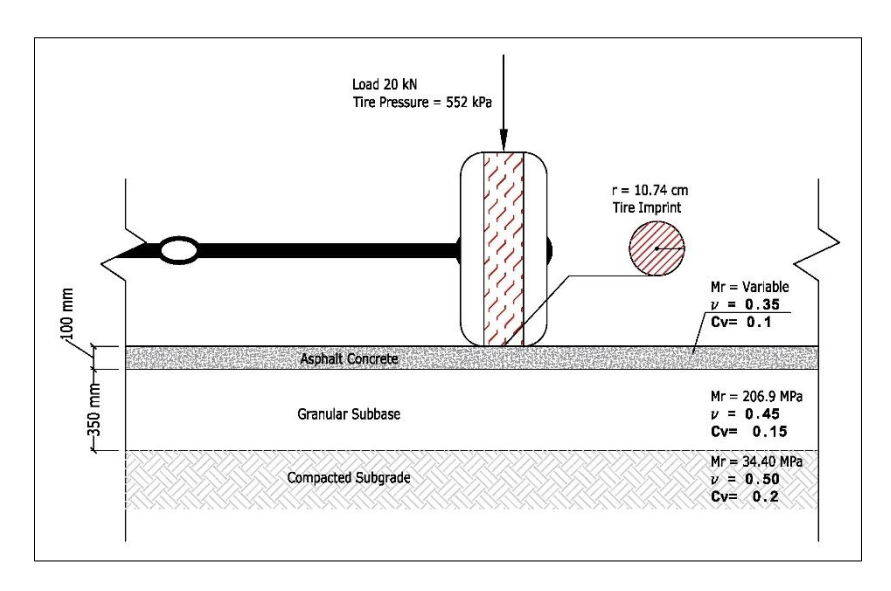


Figure 14. Analyzed pavement structure using VESY 5W

The traffic loading scenario involved 20 million ESALs over a 20-year design life (1 million ESALs per year), with a tire inflation pressure of 552 kPa and a contact radius of 10.74 cm. For the rutting model, the software utilizes material-specific constants μ and α : where α reflects the rate of decrease in permanent strain with repeated loading (slope), and μ represents the proportionality between permanent and elastic strain. Fatigue cracking predictions were made using the constants k_1 and k_2 derived from the flexural fatigue model (Table 13).

The rutting behavior of asphalt concrete under cyclic loading is governed by the following relationship:

$$\frac{\Delta \epsilon_p (N)}{\epsilon} = \mu | N^{-\alpha} \tag{3}$$

where $\Delta \epsilon_p$ (N) is the vertical permanent strain at load repetition N, ϵ is the peak haversine load strain for a load pulse of 0.1 sec duration, and μ and α are material constants influenced by stress state and temperature.

The layer rutting model, which computes the cumulative rut depth from each pavement layer, is expressed as:

$$R_{D} = \int_{N_{1}}^{N_{2}} U_{s} + \frac{\varepsilon_{t}}{\varepsilon_{s}} \mu_{sub} N^{-\alpha_{sub}} + \sum_{i=1}^{n-1} \int_{N_{1}}^{N_{2}} (U_{i}^{+} - U_{i}^{-}) \mu_{i} N^{-\alpha_{i}}$$

$$\tag{4}$$

where ε_t is the strain at the top of the subgrade due to axle groups, ε_s is the strain due to a single axle, Us is the deflection at top of subgrade due to single axle load, and Ui (-) and (+) are the deflections at the top and bottom of layer i due to axle group, respectively, and μ_i , α_i are the deformation parameters for layer i.

The system rutting model treats the entire pavement as a single unit, with rutting depth given by:

$$R_D = \int_{N_1}^{N_2} U \,\mu_{sys} \, N^{-\alpha_{sys} \, dN} \tag{5}$$

where U is the pavement surface deflection, μ_{sys} and α_{sys} is the equivalent permanent deformation parameters.

Figures 15 to 17 display the predicted rut depth, cracking index, and Present Serviceability Index (PSI) over the service life. Figure 15 displays the rut depth progression over time. The reference binder (RB) exhibits rapid rutting, exceeding the critical 13 mm limit before the 6th year. PMB also fails to meet long-term rutting resistance, surpassing the threshold before year 10. In contrast, all CNT-modified mixes remained under the 13 mm threshold throughout the 20-year period. Notably, PCNT2.0% demonstrated the best rutting resistance, followed closely by PCNT1.5% and PCNT1.0%.

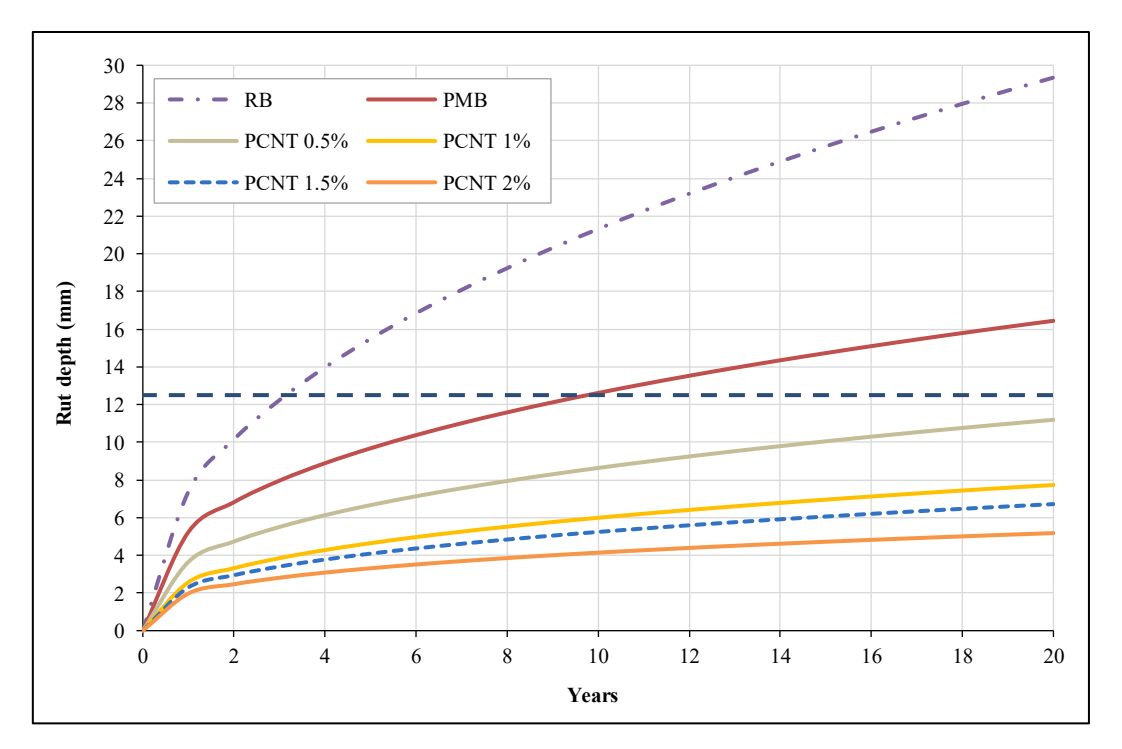


Figure 15. Rut depth versus pavement service life

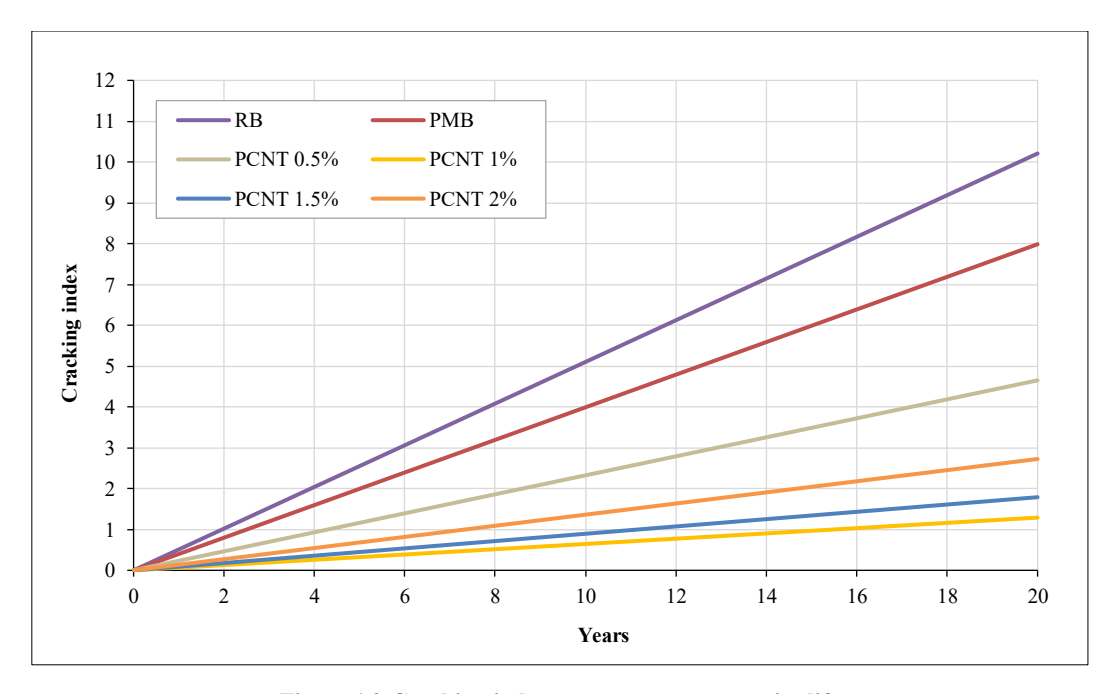


Figure 16. Cracking index versus pavement service life

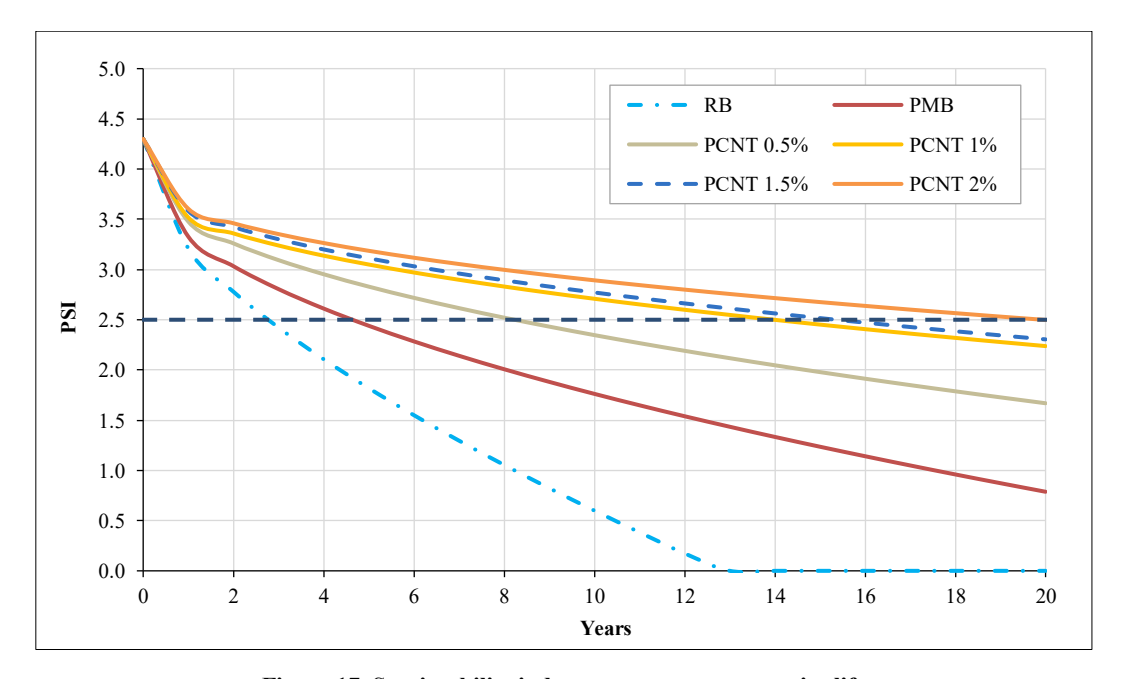


Figure 17. Serviceability index versus pavement service life

Figure 16 shows the cracking index (CI), where lower values indicate better fatigue resistance. PCNT1.0% clearly outperforms all other mixes, maintaining the lowest CI throughout design life. This is especially significant compared to PCNT2.0%, which despite excellent rutting performance exhibited relatively higher cracking index values, indicating more susceptibility to fatigue damage. Figure 17 illustrates the Present Serviceability Index (PSI) as a function of pavement service life for the different binder formulations. The mix with the reference binder (RB) exhibited the most rapid deterioration, with PSI dropping below the critical threshold of 2.5 by year 3, indicating early functional failure. The PMB mix showed modest improvement, maintaining PSI ≥ 2.5 for 5 years. The incorporation of CNTs led to substantial gains in long-term durability. PCNT0.5% sustained acceptable serviceability for 8 years, while PCNT1.0% and PCNT1.5% extended this period to 14 and 15 years, respectively. Notably, PCNT2.0% maintained PSI above 2.5 throughout the full 20-year design life, indicating superior resistance to surface degradation predominantly caused by rutting. However, as discussed in Figure 17, PCNT2.0% exhibited a higher cracking index than PCNT1.0%, suggesting relatively lower resistance to fatigue-induced damage. The VESYS analysis underscores the performance benefits of CNT-modified asphalt binders. While PCNT2.0% delivered the most favorable outcomes in terms of rutting and serviceability, PCNT1.0% achieved the most balanced performance, demonstrating good resistance to rutting as well as superior fatigue cracking. These findings support the effectiveness of combined PE/CNT modification in enhancing the long-term performance and sustainability of flexible pavement systems.

4. Conclusions

This study investigated the performance of asphalt binder and mixtures when modified with polyethylene (PE) and varying dosages of carbon nanotube (CNT). The asphalt binder was modified by 4.0% PE and four dosages of CNT which are 0.5%, 1.0%, 1.5%, and 2.0%. The addition effect was evaluated through series of laboratory tests including conventional tests and rheological test for binder. For the mixture's evaluation, Marshall stability and flow and their volumetric properties, rutting, stiffness and fatigue tests. Finally, a pavement performance prediction was made using VESYS 5W. From the results achieved the following conclusions can be drawn:

- The combined addition of PE and CNT has significantly enhanced the overall performance of asphalt binder and mixtures. The addition of 1% CNT with the 4% PE showed best test results which reflect to good performance.
- The asphalt cement penetration was decreased when the CNT dosages were increased which indicate a stiffening effect while the softening point gained an opposite performance.
- The addition of PE to asphalt binder increased the viscosity by 1468% compared to reference binder and when incorporating the CNT, it was noticed that the viscosity is decreased.
- The failure temperature was increased in estimating the high temperature performance grade of the binder when adding the modifiers. The 1% CNT achieved the highest pass/fail temperature of high temperature PG which is increased by around 10% compared to the reference binder
- The asphalt mixtures with 2% CNT (PCNT2%) have the most resistance to permanent deformation when tested under repeated load which was increased by around one-third of the permanent strain at reference binder. This can mainly be attributed to the reinforcement effect obtained through the CNT incorporation.
- High resilient modulus value (Mr) and most balanced fatigue resistance were achieved through using 1.0% CNT.
- The PCNT1.0% blend achieved the best balance of performance, showing good rutting resistance and excellent fatigue cracking resistance.

Finally, according to the laboratory results achieved in this research, it can be said the use of PE/CNT in modifying asphalt binder is reasonably beneficial to the performance. However, it highly recommended to validate these results with large-scale testing sections.

5. Declarations

5.1. Author Contributions

Conceptualization, A.A.; methodology, A.A. and H.A.; software, A.M.; validation, A.F. and M.M.; formal analysis, A.A. and H.A.; investigation, A.M.; resources, A.M. and A.F.; data curation, A.A. and A.M.; writing—original draft preparation, A.A. and H.A.; writing—review and editing, H.A.; visualization, A.A. and M.M.; supervision, A.A.; project administration, A.A.; funding acquisition, A.A., H.A., and A.F. All authors have read and agreed to the published version of the manuscript.

5.2. Data Availability Statement

The data presented in this study are available in the article.

5.3. Funding

The authors received no financial support for the research, authorship, and/or publication of this article.

5.4. Conflicts of Interest

The authors declare no conflict of interest.

6. References

- [1] Elwardany, M. D., Planche, J. P., & King, G. (2022). Proposed Changes to Asphalt Binder Specifications to Address Binder Quality-Related Thermally Induced Surface Damage. Transportation Research Record, 2676(5), 176–191. doi:10.1177/03611981211065428.
- [2] Yang, K., Cui, H., Ma, X., & Zhu, M. (2023). Understanding and characterizing the fatigue cracking resistance of asphalt binder at intermediate temperature: A literature review. Construction and Building Materials, 407, 133432. doi:10.1016/j.conbuildmat.2023.133432.
- [3] Albayati, A. H., Mustafa, F. S., Al-ani, A. F., Sukhija, M., Moudhafar, M. M., & Maher, A. M. (2025). Advancing asphalt binder performance through nanomaterial and polymer modification: Experimental and statistical insights. Results in Engineering, 25, 104458. doi:10.1016/j.rineng.2025.104458.

[4] Yang, Q., Lin, J., Wang, X., Wang, D., Xie, N., & Shi, X. (2024). A review of polymer-modified asphalt binder: Modification mechanisms and mechanical properties. Cleaner Materials, 12, 100255. doi:10.1016/j.clema.2024.100255.

- [5] Emtiaz, M., Imtiyaz, M. N., Majumder, M., Idris, I. I., Mazumder, R., & Rahaman, M. M. (2023). A Comprehensive Literature Review on Polymer-Modified Asphalt Binder. CivilEng, 4(3), 901–932. doi:10.3390/civileng4030049.
- [6] Yin, F., West, R., Powell, B., & DuBois, C. J. (2025). Short-Term Performance Characterization and Fatigue Damage Prediction of Asphalt Mixtures Containing Polymer-Modified Binders and Recycled Plastics. Transportation Research Record, 2679(1), 742–759. doi:10.1177/03611981221143119.
- [7] Jexembayeva, A., Konkanov, M., Aruova, L., Kirgizbayev, A., & Zhaksylykova, L. (2024). Performance Optimization Approach of Polymer-Modified Asphalt Mixtures with PET and PE Waste. Polymers, 16(23), 3308. doi:10.3390/polym16233308.
- [8] Li, M., Luo, C., Zhu, L., Cong, P., Li, H., Chen, X., Zhang, Y., Chao, M., & Yan, L. (2023). Polyethylene based on molecular weight design for eco-friendly asphalt. Journal of Applied Polymer Science, 140(26), 53994. doi:10.1002/app.53994.
- [9] Ma, J., Sandrasagra, J., Oriotis, N., & Hesp, S. A. M. (2024). Evaluating the phase compatibility of asphalt binders using modulated differential scanning calorimetry. Bituminous Mixtures and Pavements VIII, 47–54, Boca Raton, United States. doi:10.1201/9781003402541-6.
- [10] Tang, J., & Wang, H. (2023). Compatibility and Self-Healing Properties of Asphalt Binder with Polyethylene Plastics: Observations from Coarse-Grained Molecular Simulation. Journal of Materials in Civil Engineering, 35(11), 4023412. doi:10.1061/jmcee7.mteng-16148.
- [11] Aljbouri, H. J., & Albayati, A. H. (2023). Effect of nanomaterials on the durability of hot mix asphalt. Transportation Engineering, 11, 100165. doi:10.1016/j.treng.2023.100165.
- [12] Afshin, A., & Behnood, A. (2025). Nanomaterials in asphalt pavements: A state-of-the-art review. Cleaner Waste Systems, 10, 100214. doi:10.1016/j.clwas.2025.100214.
- [13] Eisa, M. S., Mohamady, A., Basiouny, M. E., Abdulhamid, A., & Kim, J. R. (2022). Mechanical properties of asphalt concrete modified with carbon nanotubes (CNTs). Case Studies in Construction Materials, 16, 930. doi:10.1016/j.cscm.2022.e00930.
- [14] He, Z., Ou, J., Xie, T., Yang, F., & Li, Y. (2024). Evaluation of different functionalized multi-walled carbon nanotubes (MWCNTs) modified asphalts. Archives of Civil Engineering, 70(4), 307–322. doi:10.24425/ace.2024.151894.
- [15] Sun, P., Zhang, K., Xiao, Y., & Liang, Z. (2022). Analysis of Pavement Performance for Nano-CaCO3/SBS Modified Asphalt Mixture. Journal of Physics: Conference Series, 012031. doi:10.1088/1742-6596/2329/1/012031.
- [16] Liz, J. V. de, Barra, B. S., Mikowski, A., Hughes, G., & Pérez, Y. A. G. (2024). Trends in the incorporation of nanomaterials in asphalt binders to improve rheological properties. Cademo Pedagógico, 21(9), e8183. doi:10.54033/cadpedv21n9-256.
- [17] Lu, Y., Li, S., Jiang, Y., Yang, X., & Li, L. (2024). Rheological and Aging Properties of Nano-Clay/SBS Composite-Modified Asphalt. Materials, 17(17), 4376. doi:10.3390/ma17174376.
- [18] Salam, K., Mir, M. S., & Mohanty, B. (2024). Rheological Investigation of Nano Silica-SBS Modified Soft Grade Bitumen. Transportation Research. TPMDC 2022. Lecture Notes in Civil Engineering, 434, Springer, Singapore. doi:10.1007/978-981-99-6090-3_13.
- [19] Liu, B., Li, X., & Li, S. (2024). Pavement performance analysis of carbon nanotube/SBS composite modified asphalt. Carbon Letters, 34(1), 343-350. doi:10.1007/s42823-023-00605-0.
- [20] Huang, H., Wang, Y., Wu, X., Zhang, J., & Huang, X. (2024). Nanomaterials for Modified Asphalt and Their Effects on Viscosity Characteristics: A Comprehensive Review. Nanomaterials, 14(18), 1503. doi:10.3390/nano14181503.
- [21] Xin, X., Yao, Z., Shi, J., Liang, M., Jiang, H., Zhang, J., Zhang, X., & Yao, K. (2020). Rheological properties, microstructure and aging resistance of asphalt modified with CNTs/PE composites. Construction and Building Materials, 262, 120100. doi:10.1016/j.conbuildmat.2020.120100.
- [22] Li, J., & Tang, F. (2023). Effects of two metal nanoparticles on performance properties of asphalt binder and stone matrix asphalt mixtures containing waste high density polyethelene. Construction and Building Materials, 401, 132787. doi:10.1016/j.conbuildmat.2023.132787.
- [23] Liang, M., Su, L., Li, P., Shi, J., Yao, Z., Zhang, J., Jiang, H., & Luo, W. (2020). Investigating the rheological properties of carbon nanotubes/polymer composites modified asphalt. Materials, 13(18), 4077. doi:10.3390/ma13184077.